Aminal linked inorganic-organic hybrid nanoporous materials (HNMs) for CO_2 capture and H_2 storage applications

Raeesh Muhammad, Pawan Rekha and Paritosh Mohanty*

Department of Chemistry, Indian Institute of Technology Roorkee, Roorkee, Uttarakhand - 247667, INDIA

*Email: pmfcy@iitr.ac.in, paritosh75@gmail.com

FT-IR and NMR spectroscopic investigation of compound-I

FT-IR: 1702 cm^{-1} (C=O), 1570 cm^{-1} (aromatic C=C), 1209 and 1160 cm^{-1} (P=N), 1015 cm^{-1} (P-O-C)

^{1}H NMR (400 MHz, $CDCl_3$, 298 K): δ 9.95 (s, COH), 7.75 (d, Ar−H), 7.17 (d, Ar−H)

^{13}C NMR (100 MHz, $CDCl_3$, 298 K): δ 190 (C=O), δ 155 (ArCO), δ 134 (ArCH), δ 132 (ArCH) and δ 122 (ArC)

^{31}P NMR (161 MHz, $CDCl_3$, 298 K): δ 7.04 (s)

Elemental analysis: Theoretical formula: $C_{42}H_{30}N_3O_{12}P_3$

C, 58.55; H, 3.51; N, 4.88

Experimentally observed formula:

C, 58.09; H, 3.50; N, 4.85

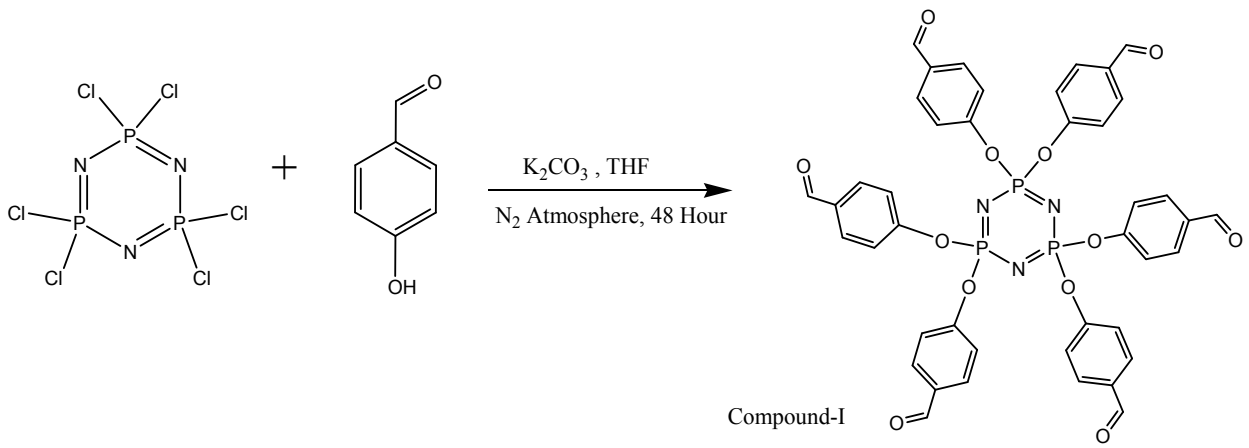

Scheme S1: Reaction scheme for the synthesis of compound - I.

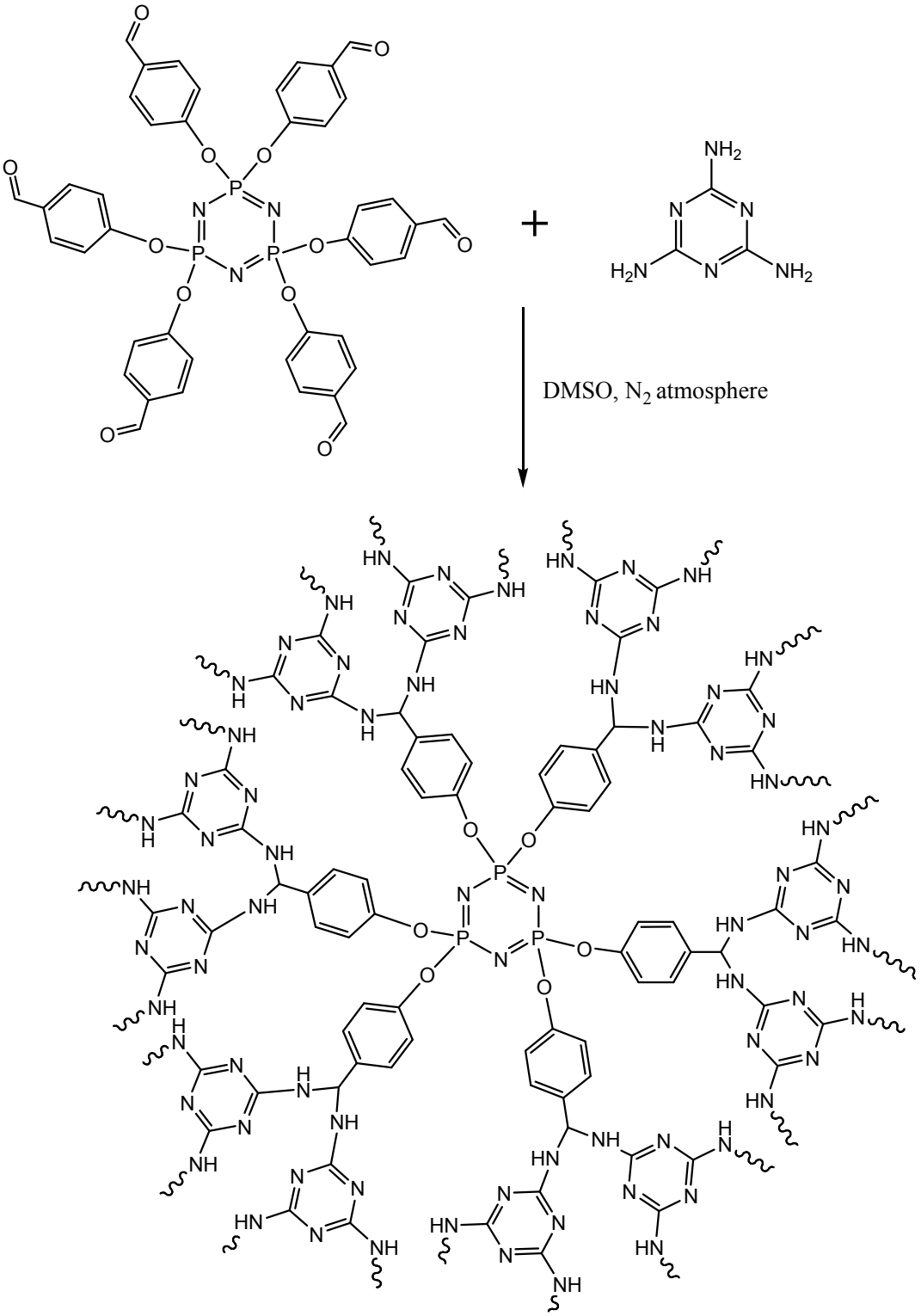

Scheme S2: Reaction scheme for the synthesis of HNMs.

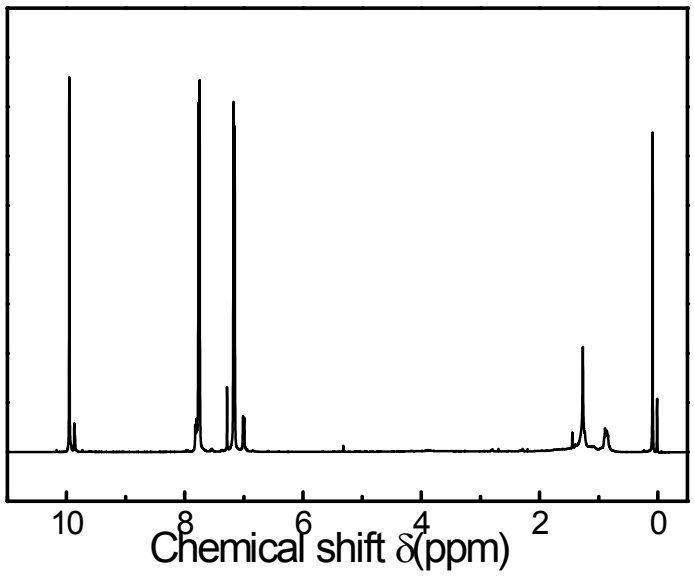

Figure S1: ^{1}H NMR spectrum. ^{1}H NMR spectrum of compound-I collected in $CDCl_3$.

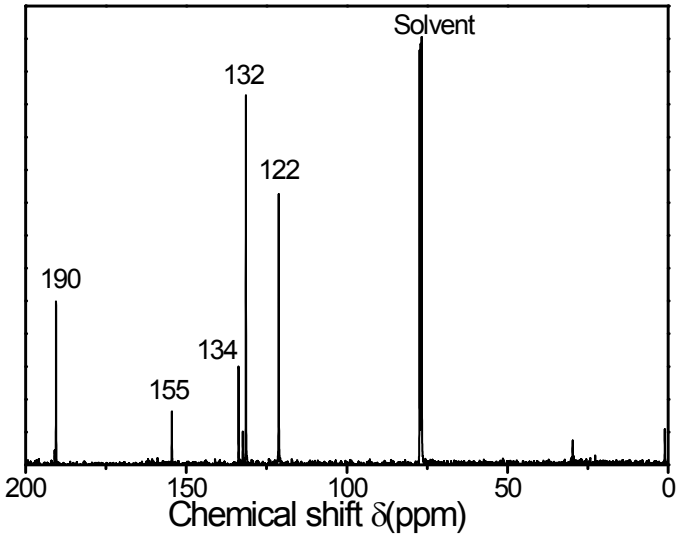

Figure S2: ^{13}C NMR spectrum. ^{13}C NMR spectrum of compound-I collected in $CDCl_3$.

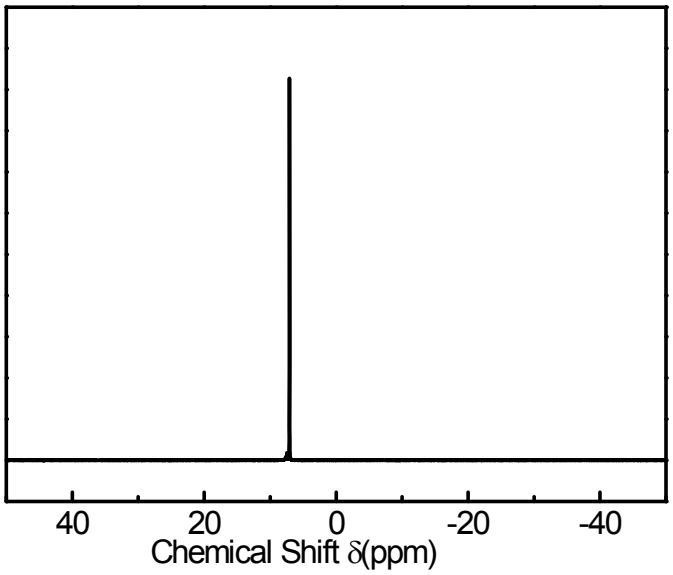

Figure S3: ^{31}P NMR spectrum. ^{31}P NMR spectrum of compound-I collected in $CDCl_3$.

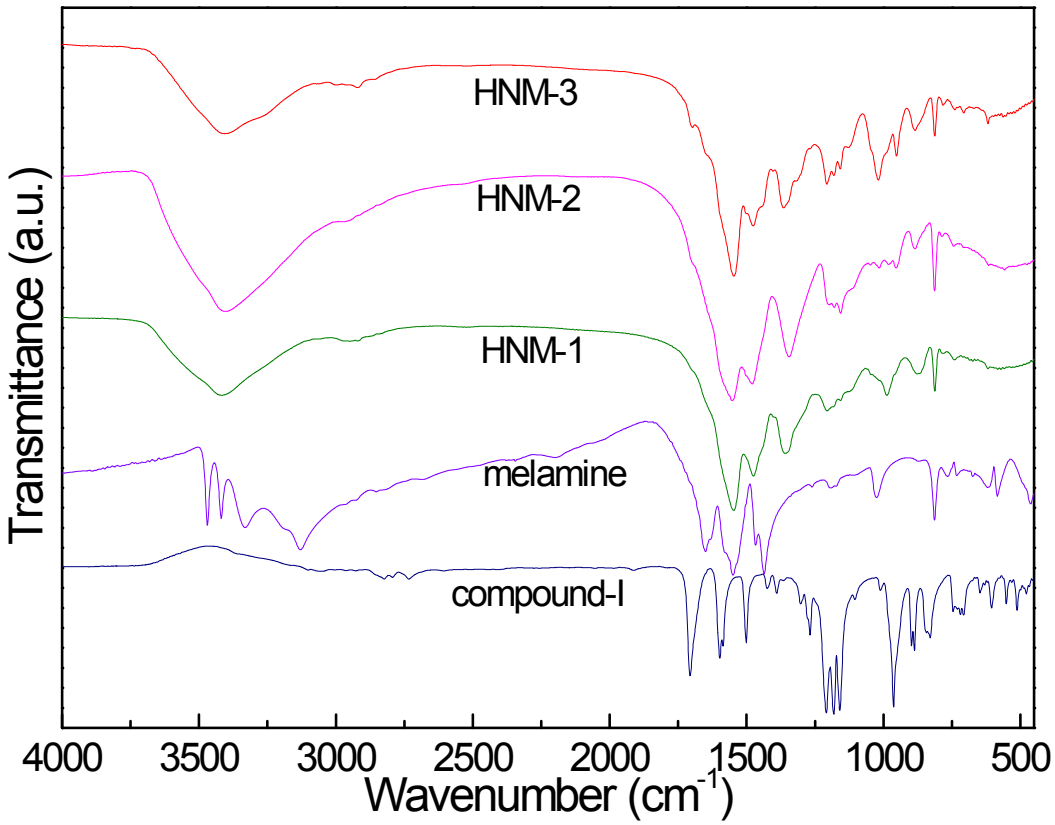

Figure S4: FT-IR spectra

Table S1: Assignment of FT-IR Bands

Bands (cm^{-1})	Assignment	*References*
3420	Aminal N-H stretching	S2, S3
2930	Aliphatic C-H stretching	S2, S3
1650	NH_2 deformation band	S2, S3
1600	C=C aromatic ring stretching	S2, S3, S4
1550	quadrant stretching of s-triazine ring	S2
1480	semicircle stretching of s-triazine ring	S2
1360	Ring and side chain CN stretching	S3
1200-1160	$_{vas}$(P=N–P),	S1
960	ν_{as}(P-O-P) vibration	S1, S6
814	Ring breathing ring def. (out of plane)	S2
520	δ(P=N-P) vibration	S1, S6

Table S2 (a): Assignment of ^{13}C CP-MAS NMR resonance signals for HNM-1

Peaks (ppm)	Assignment	*References*
166	C of triazine ring (C-1)	S2
155	C of benzene ring (C-2)	S1
135	C of benzene ring (C-3)	S3, S4
131	C of benzene ring (C-4)	S3, S4
120	C of benzene ring (C-5)	S3
55	tertiary carbon (C-6)	S2, S5

Table S2 (b): Assignment of ^{31}P CP-MAS NMR resonance signal for HNM-1

Peaks (ppm)	Assignment	*References*
9.6	P of PNC moiety	S1

Table S3: Elemental Analysis for HNMs

Calculated for $C_{78}H_{66}N_{75}O_3P_3$; N: 46.84, C: 41.77, H: 2.97, O: 4.28, P: 4.14.

Sample ID	Observed			
	N	C	H	O
HNM-1	42.16	40.18	4.46	5.25
HNM-2	41.14	40.28	5.69	5.52
HNM-3	36.13	31.78	6.20	6.23

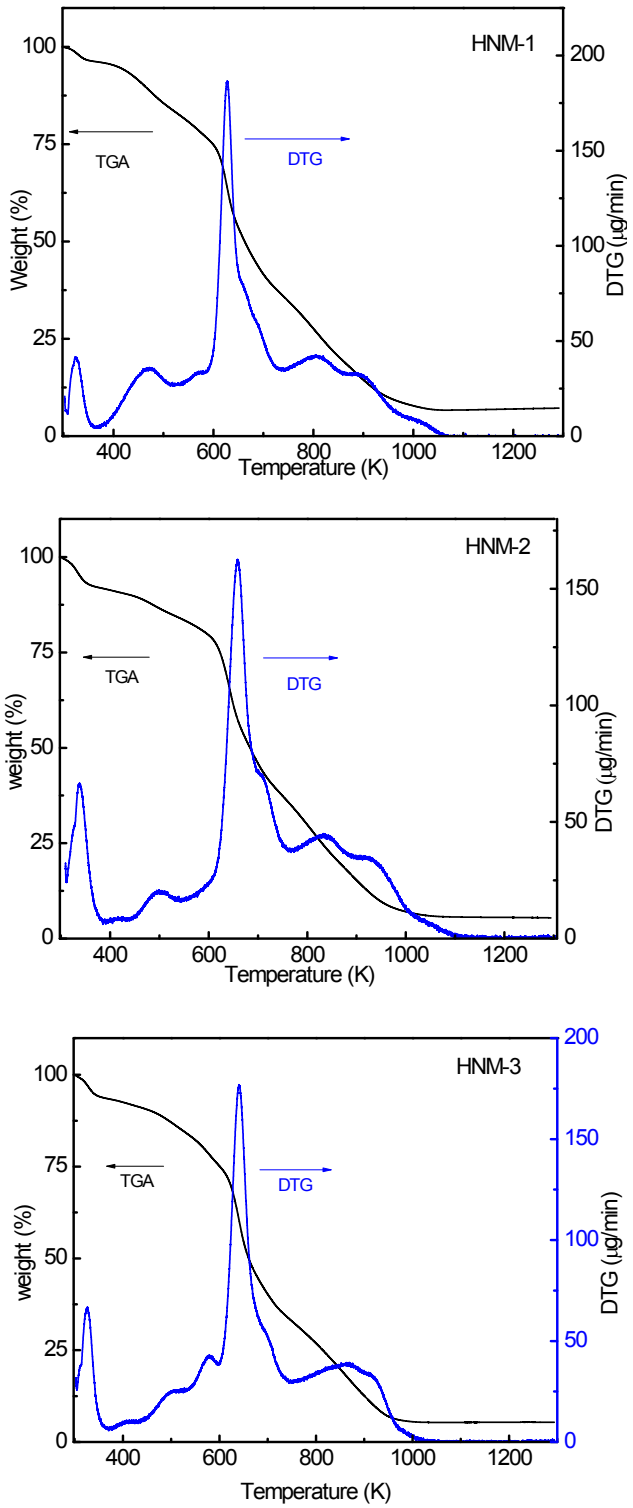

Figure S5: HNMs thermogravimetry thermograms measured in air. TGA and DTG thermograms of (a) HNM-1, (b) HNM-2 and (c) HNM-3 measured in air with a heating rate of 5 K/min.

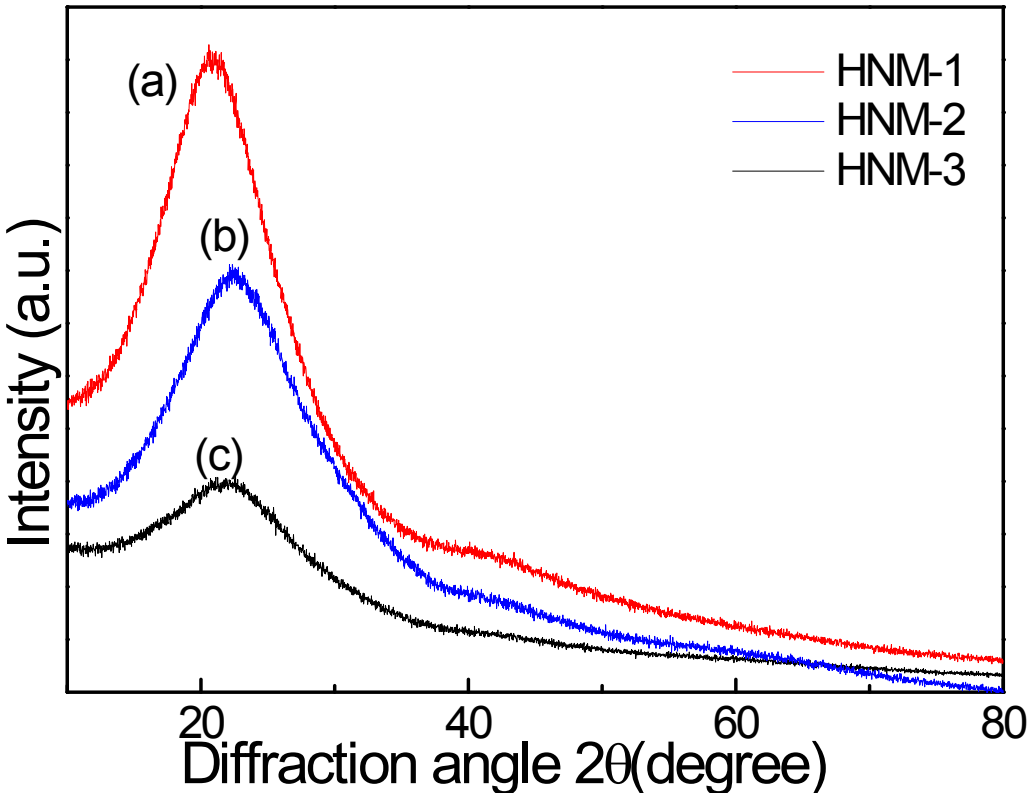

Figure S6: XRD spectra of HNMs. X-ray diffraction patterns of (a) HNM-1, (b) HNM-2 and (c) HNM-3.

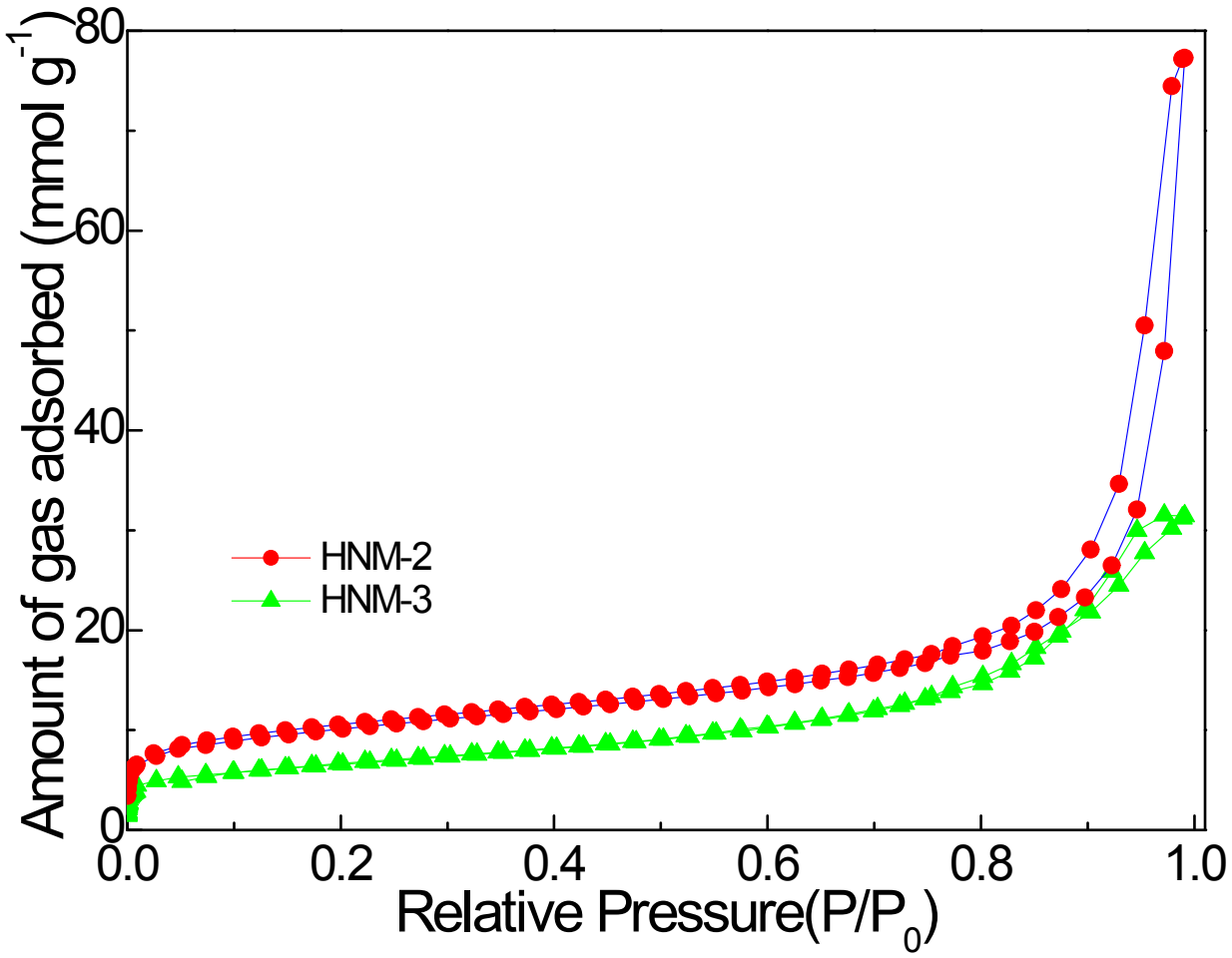

Figure S7: N_2 sorption isotherm; N_2 sorption isotherm of HNM-2 and HNM-3, measured at 77 K.

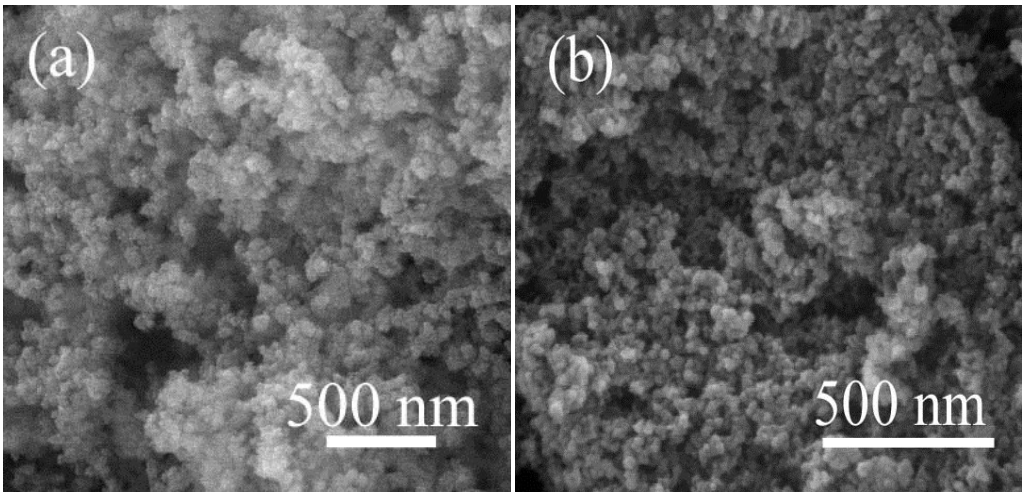

Figure S8: (a) and (b) FE-SEM image of HNM-2 and HNM-3, respectively.

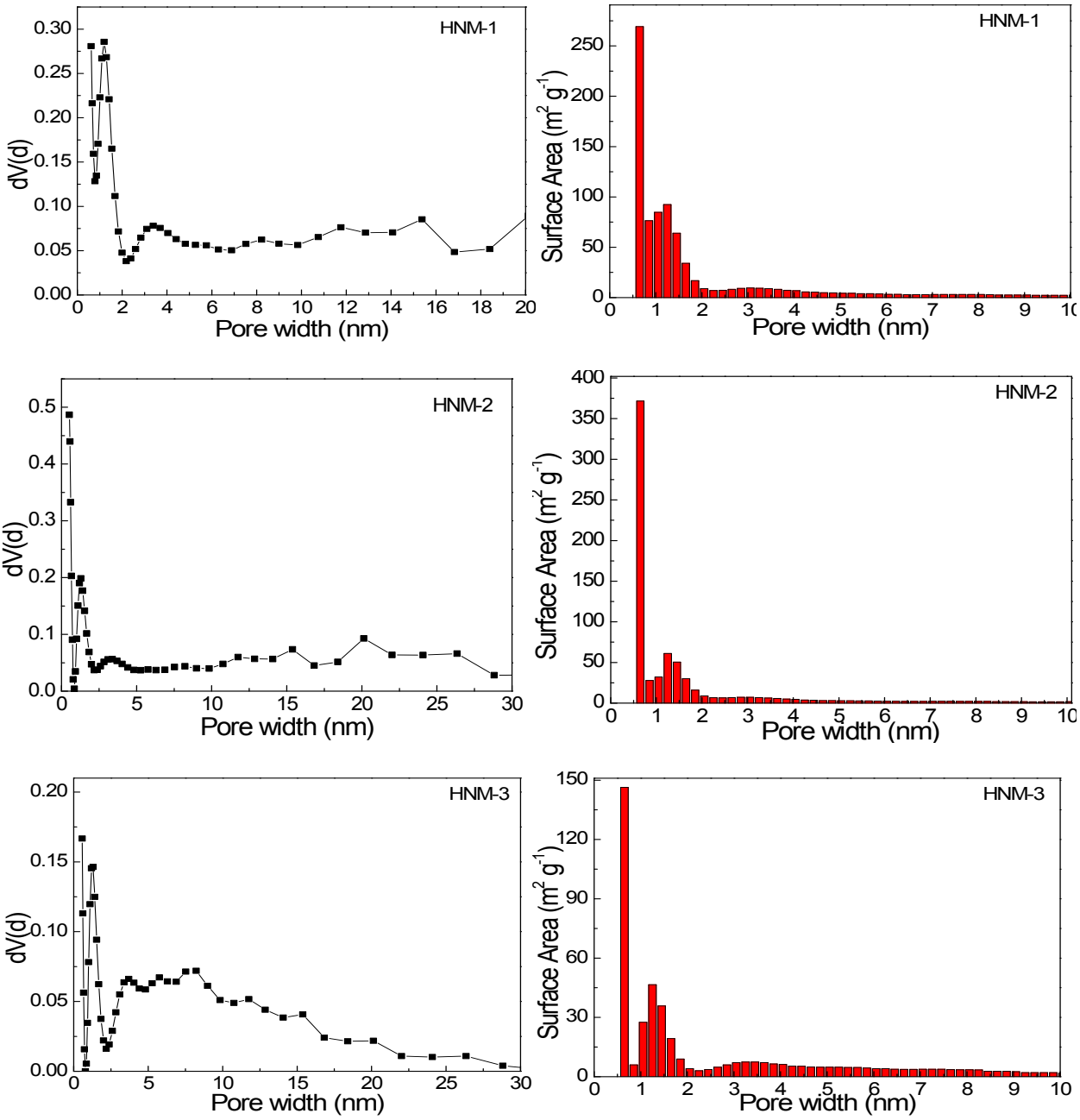

Figure S9: DFT pore size distribution of HNMs. Pore size distribution of HNM-1, HNM-2 and HNM-3 calculated from the N_2 sorption isotherm measured at 77 K using the Density Functional Theory (DFT) method.

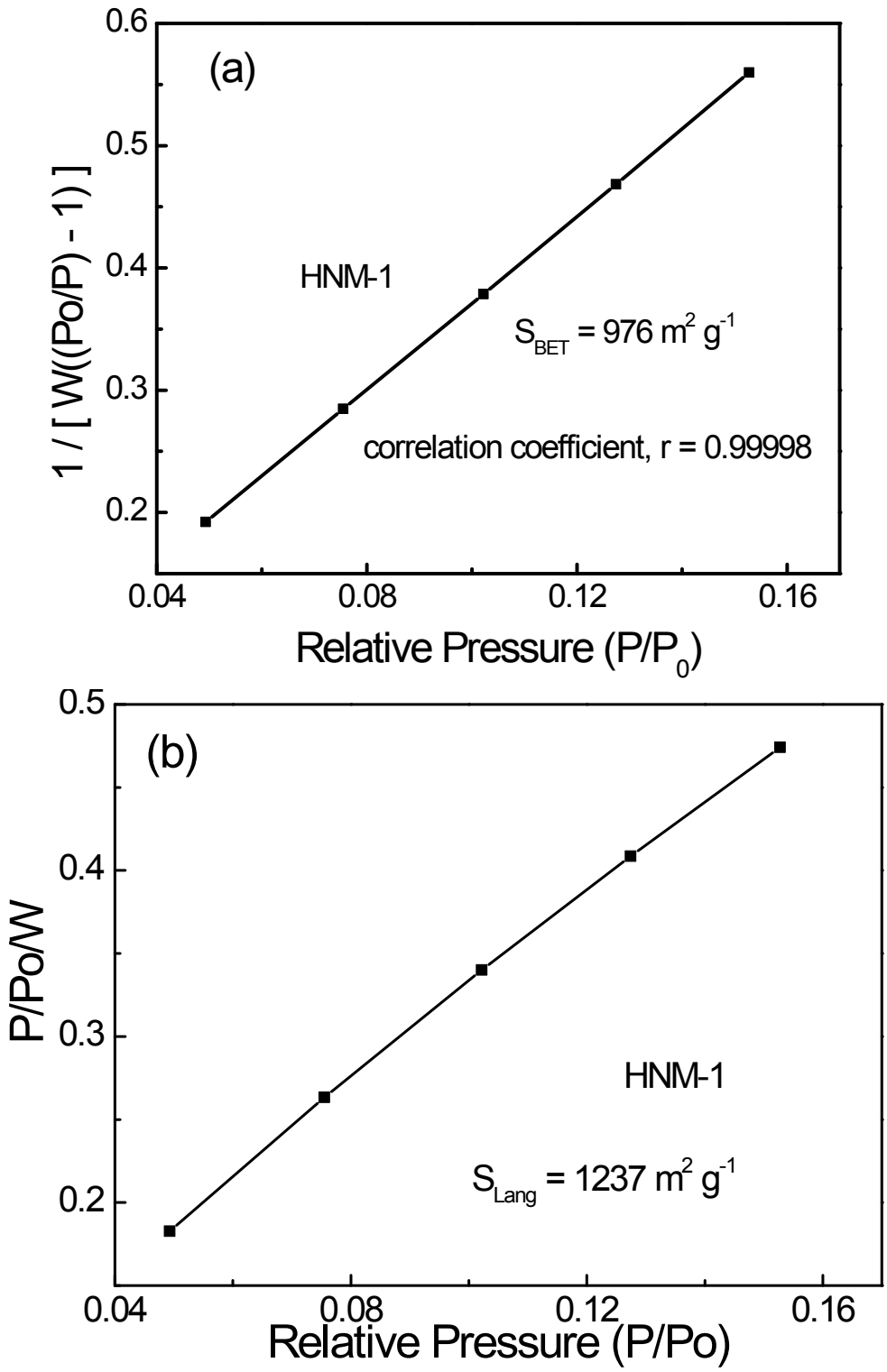

Figure S10: Multi-Point BET plot and Langmuir plot. (a) Multi-Point BET plot of HNM-1 and (b) Langmuir plot of HNM-1 calculated from the N_2 isotherm measured at 77 K.

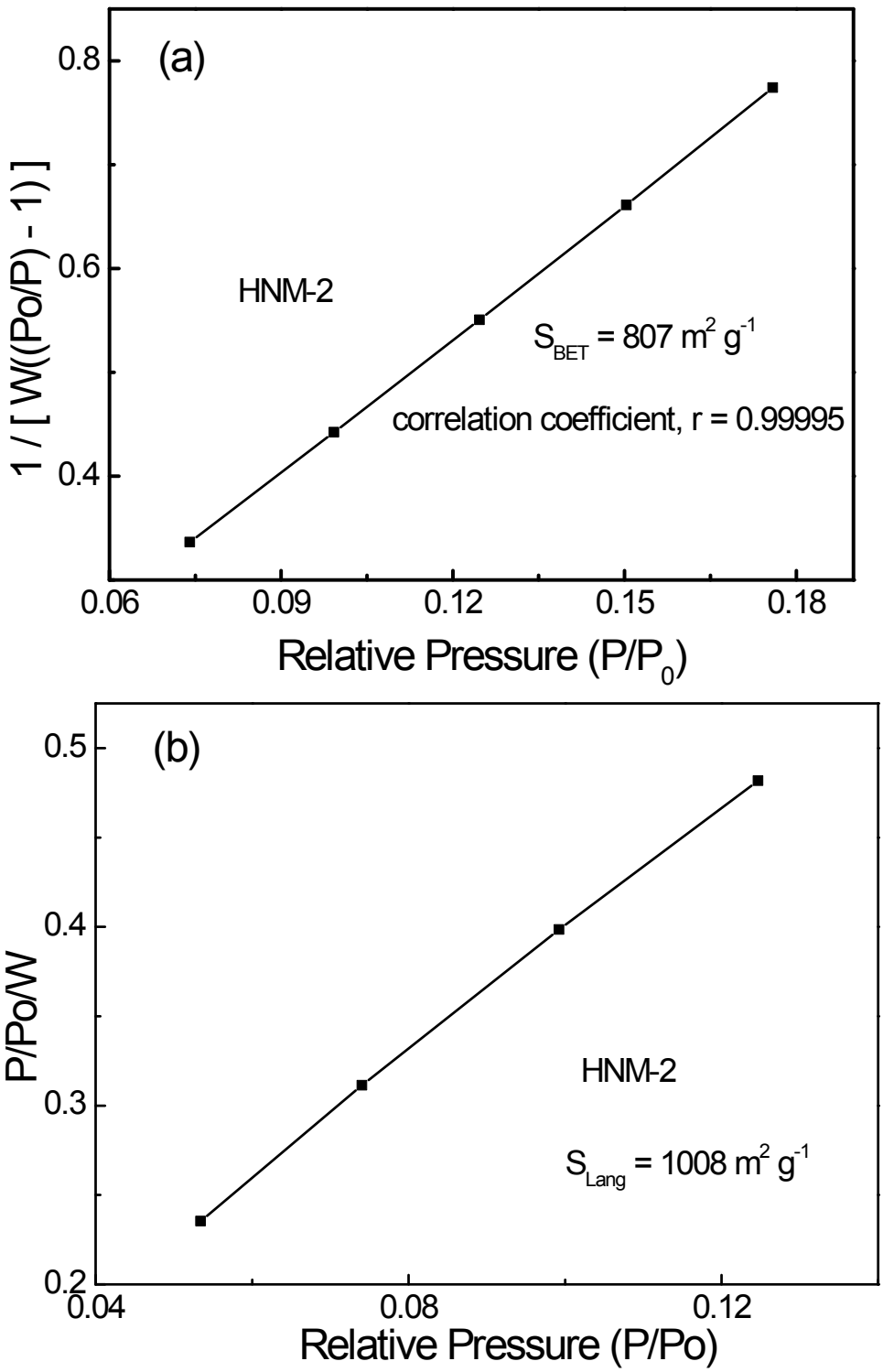

Figure S11: Multi-Point BET plot and Langmuir plot. (a) Multi-Point BET plot of HNM-2 and (b) Langmuir plot of HNM-2 calculated from the N_2 isotherm measured at 77 K.

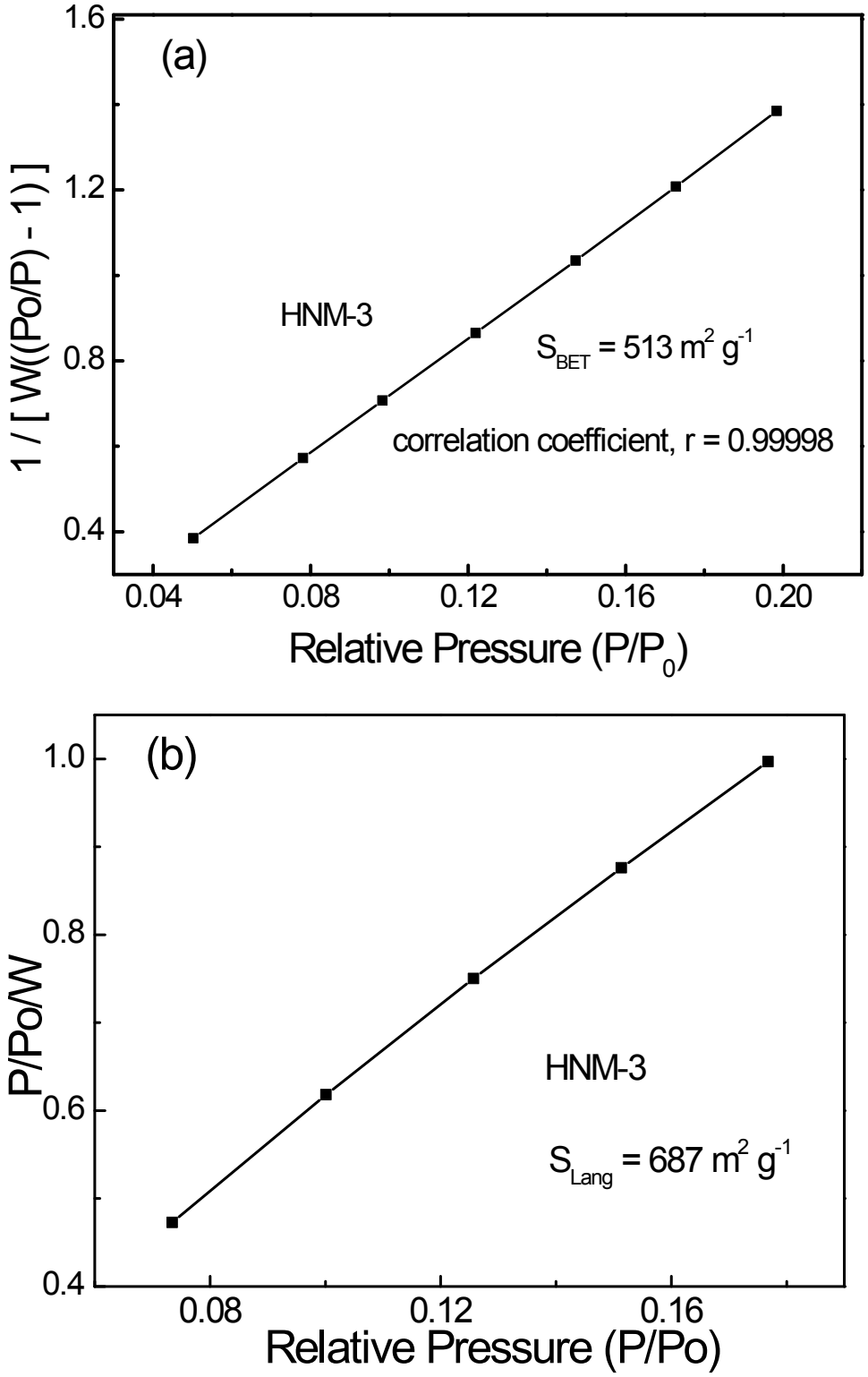

Figure S12: Multi-Point BET plot and Langmuir plot. (a) Multi-Point BET plot of HNM-3 and (b) Langmuir plot of HNM-3 calculated from the N_2 isotherm measured at 77 K.

Table-S4: Summary of Porosity and Pore Volumes for HNMs

Sample	Surface Area From N_2 Sorption at 77 K (m^2 g^{-1})			DFT and Monte-Carlo Cumulative		Total pore volume (cm^3 g^{-1})
				Surface Area (m^2 g^{-1})	Pore volume (cm^3 g^{-1})	
	BET	External Surface Area	Langmuir	N_2 at 77K	N_2 at 77K	N_2 at 77K
HNM-1	976	603	1237	967	2.11	1.05
HNM-2	807	493	969	861	1.83	0.86
HNM-3	513	403	687	517	1.03	0.67

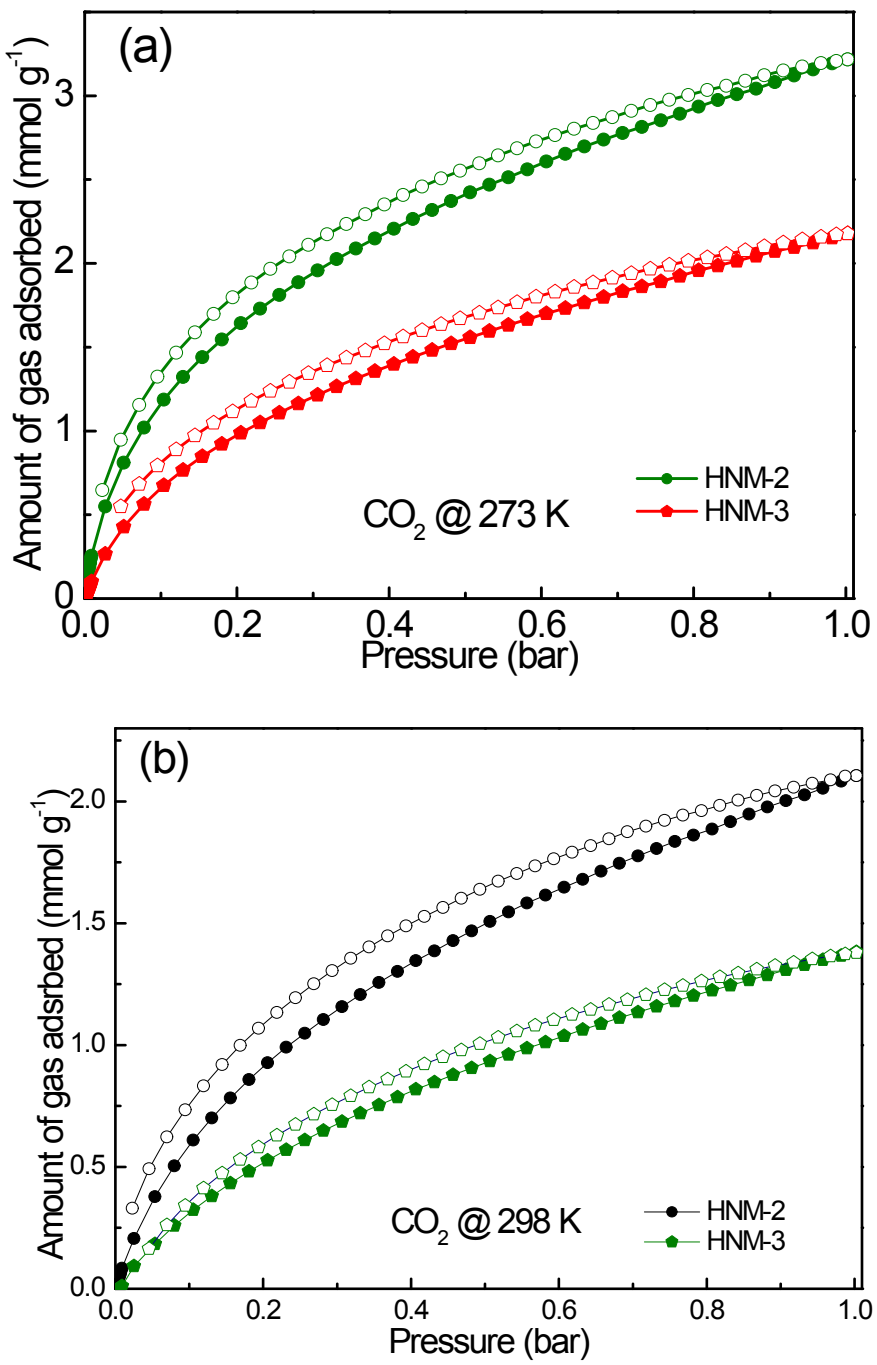

Figure S13: HNM- 2, 3 CO_2 isotherms; (a) CO_2 sorption isotherms at 273 and (b) 298 K, respectively.

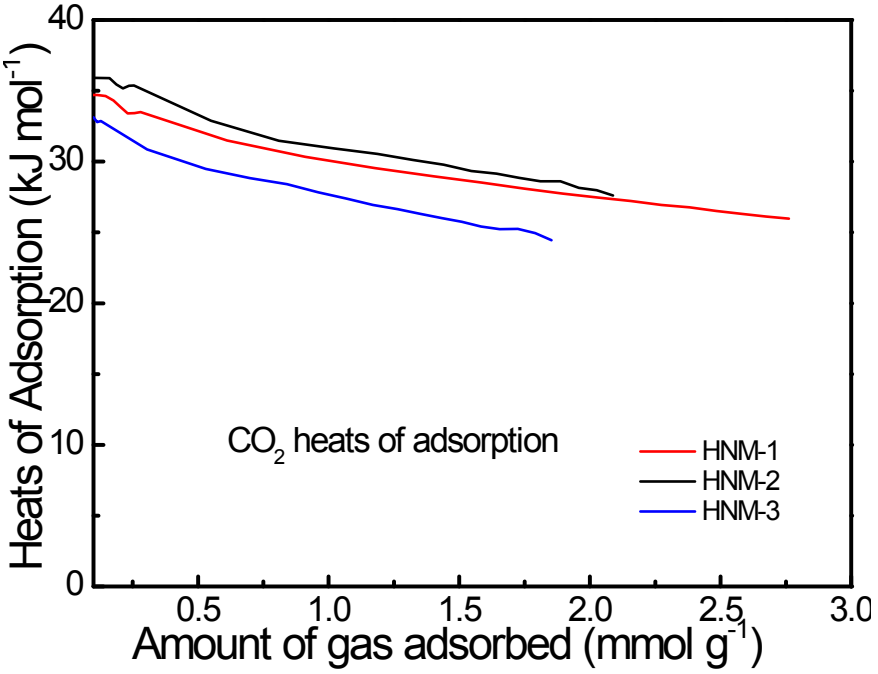

Figure S14: Isosteric heat of adsorption of HNMs. Isosteric heats of adsorption for CO_2 have been calculated from CO_2 isotherms collected at 273 and 298 K.

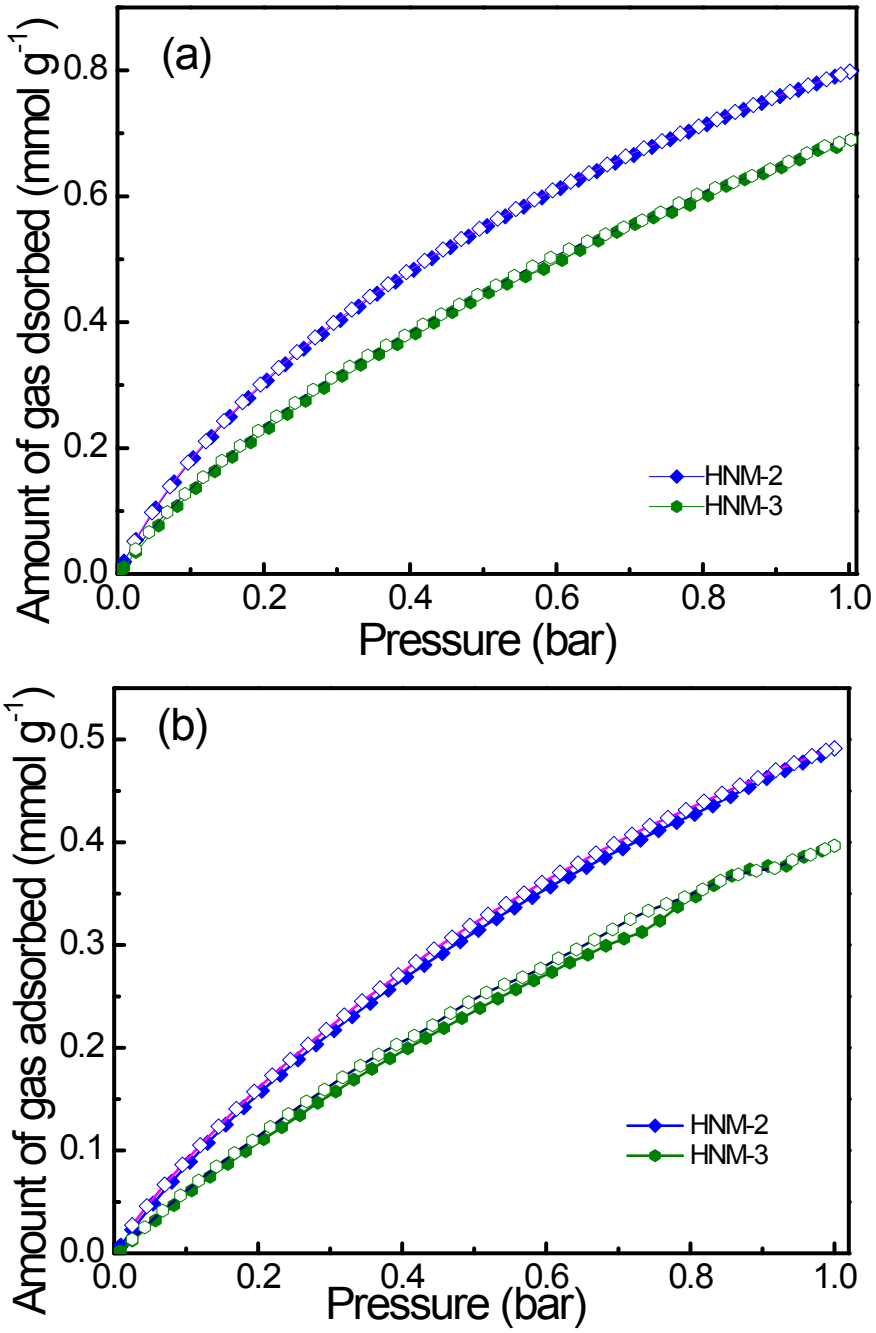

Figure S15: HNM-2, 3 CH_4 isotherms; (a) CH_4 sorption isotherms at 273 and (b) 298 K, respectively.

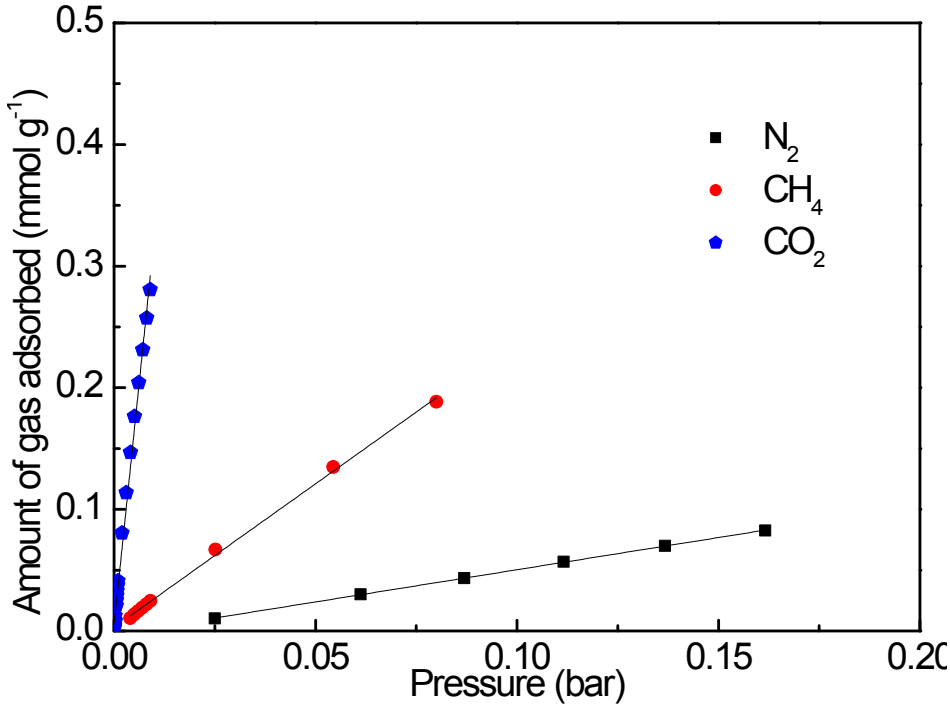

Figure S16: HNM-1 gas sorption selectivities. Selectivities of CO_2:N_2 and CO_2:CH_4 for HNM-1 at 273 K.

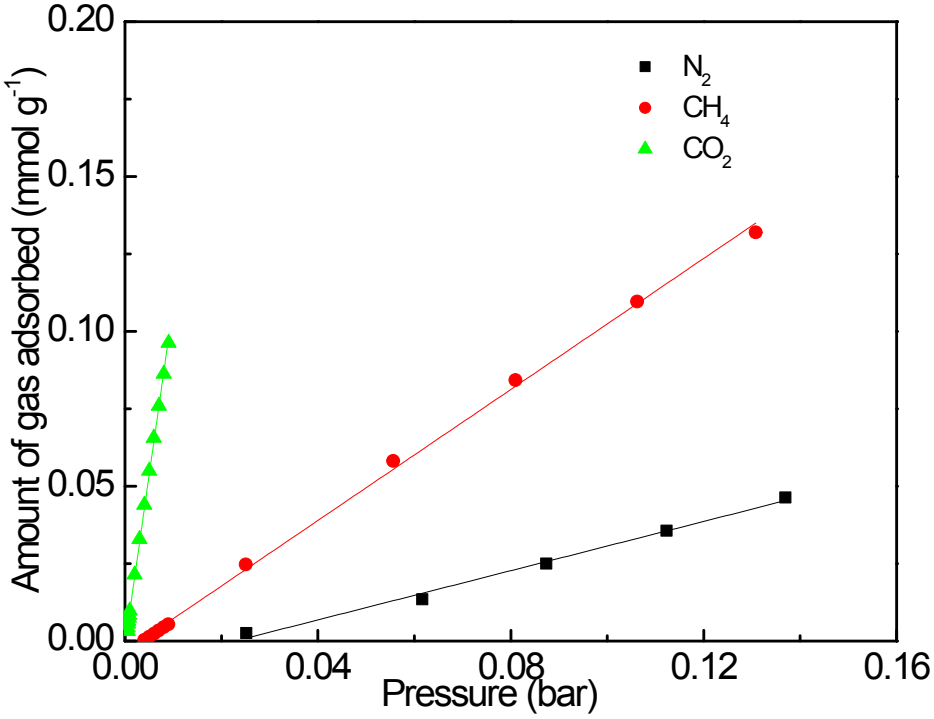

Figure S17: HNM-1 gas sorption selectivities. Selectivities of CO_2:N_2 and CO_2: CH_4 for HNM-1 at 298 K.

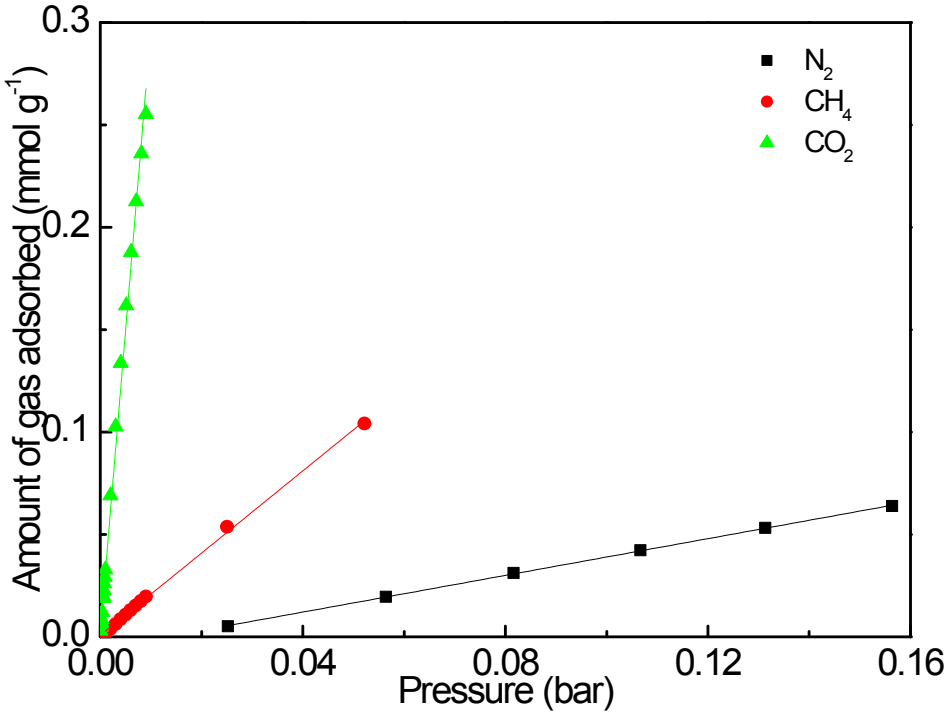

Figure S18: HNM-2 gas sorption selectivities. Selectivities of CO_2:N_2 and CO_2:CH_4 for HNM-2 at 273 K.

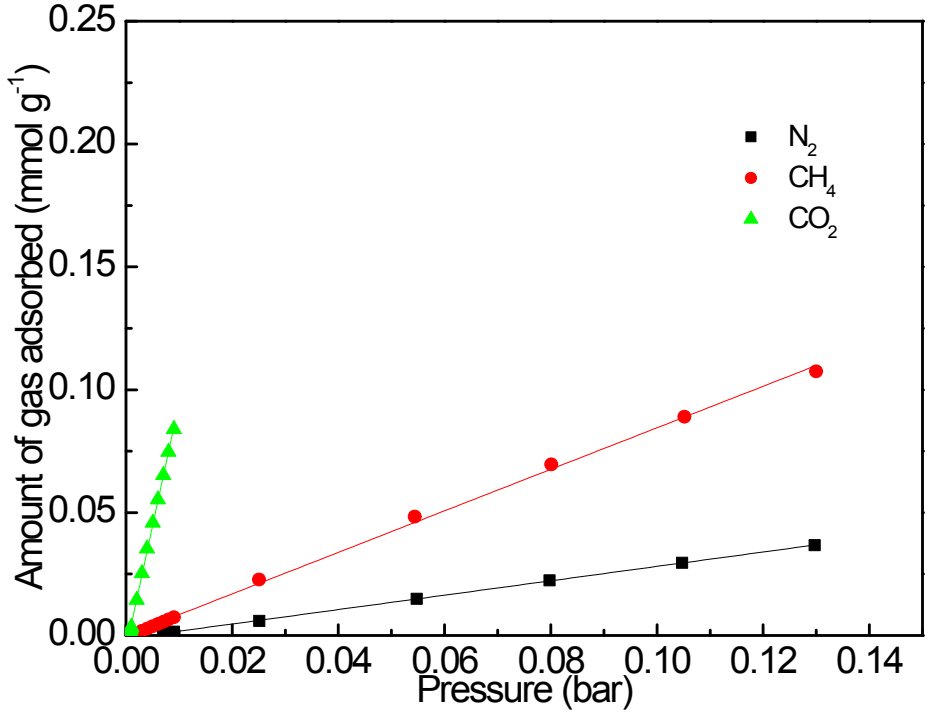

Figure S19: HNM-2 gas sorption selectivities. Selectivities of CO_2:N_2 and CO_2:CH_4 for HNM-2 at 298 K.

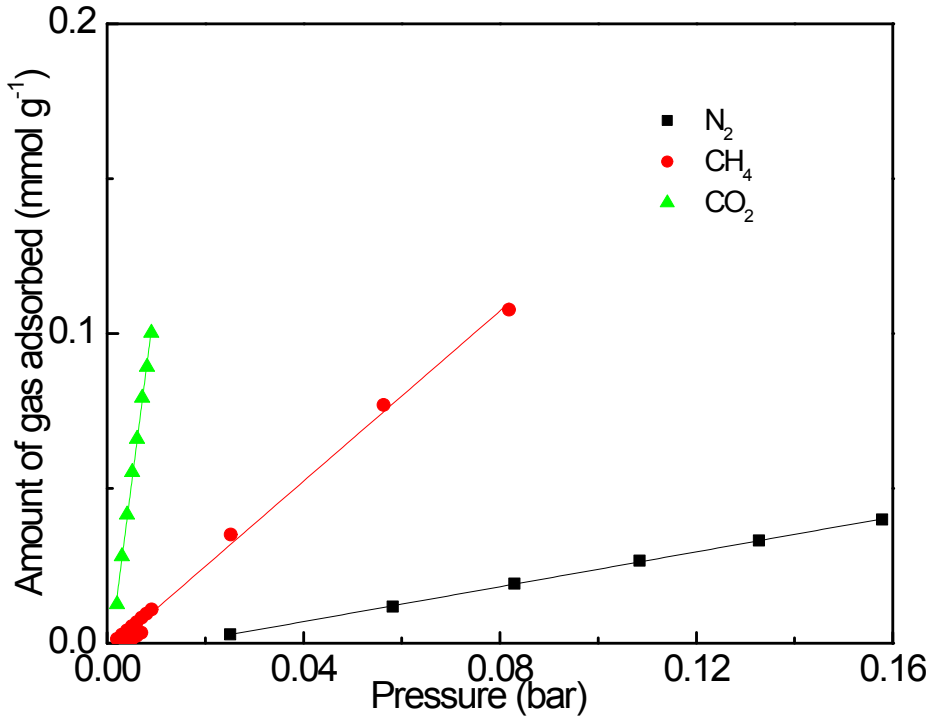

Figure S20: HNM-3 gas sorption selectivity. Selectivity of CO_2:N_2 and CO_2:CH_4 for HNM-3 at 273 K.

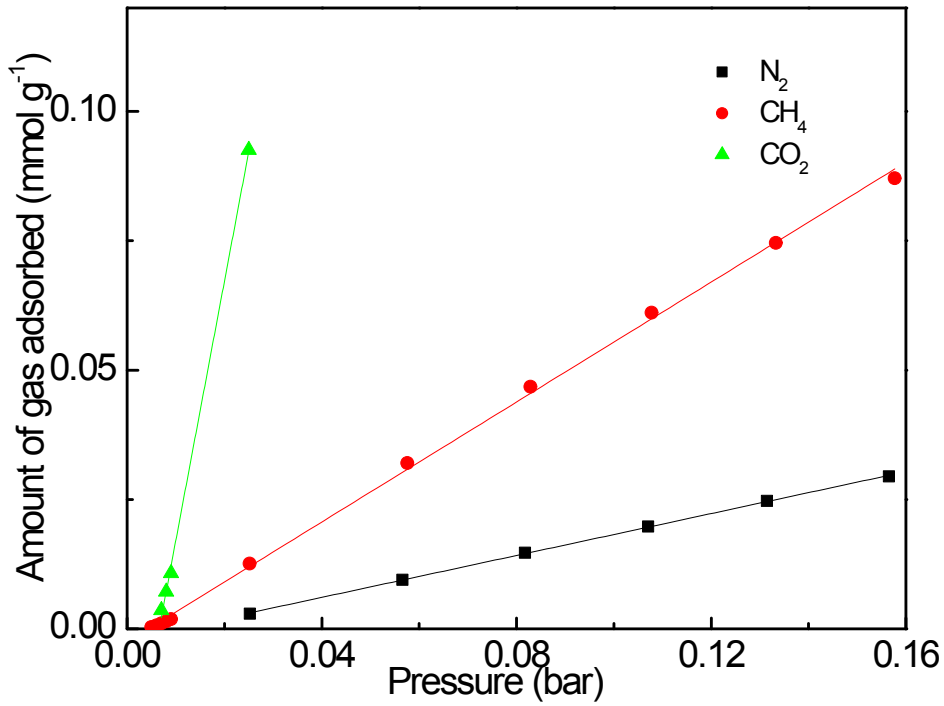

Figure S21: HNM-3 gas sorption selectivities. Selectivity of CO_2:N_2 and CO_2:CH_4 for HNM-3 at 298 K.

Table S5: Summary of gas adsorption properties of HNMs at low pressure

Sample ID	CO_2 uptake			CH_4 uptake			Selectivity				H_2 uptake[e]
	wt %[a]	wt %[b]	Q_{st}	wt %[a]	wt %[b]	Q_{st}	CO_2/N_2[c]	CO_2/CH_4[c]	CO_2/N_2[d]	CO_2/CH_4[d]	wt%
HNM-1	18.9	12.3	33.0	1.79	0.88	25.7	62	14	28	11	1.65
HNM-2	13.2	8.16	35.9	1.48	0.79	23.0	67	17	35	12	1.35
HNM-3	9.5	6.08	32.0	1.10	0.63	25.2	44	9	25	10	0.92

[a]273 K, 1 bar; [b]298 K, 1 bar; [c]273 K, 1 bar; [d]298 K, 1 bar; [e]77 K, 1 bar; unit of Q_{st}: kJ mol^{-1}. Selectivity at 273 and 298 K.

Table S6: Gas adsorption properties of selected porous materials at low pressure

Summary of gas adsorption properties of porous materials at low pressure

Sample ID	Surface Area[a]		CO_2 uptake[c]		Selectivity		Reference
	BET	Langmuir	wt %	Q_{st}	CO_2/N_2	CO_2/CH_4	
PAN-1	925	1366	14.8	36.5	61	12	S3
TBILP-1	330	-	11.7	35	63	9	S4
TBILP-2	1080	-	22.8	29	40	7	S4
APOP-3	1402	1779	19.9	27.5	27.5	5.3	S5
PHM	453	620	8.05	26	-	-	S6
PAF-3	2932	3857	15.3	19.2	87	30	S7
BLP-1(H)	1360	1744	7.4	25.3	-	-	S8
BLP-(12)H	2244	2866	12.8	25.2	-	-	S8
PECONF-3	851	969	15.35	24.9	77	10	S9
PPF-1	1740	2157	26.7	25.6	14.5 (1 bar) 273 K	11 (1 bar) 273 K	S10
BILP-4	1135	1486	23.5	28.7	79	10	S11
fl-CTF350	1235	-	18.8	32.7	27	-	S12
C-NP	946	-	13.6	28.8	29	98	S13

[a]Unit: m^2 g^{-1}. [b]Unit: cm^3 g^{-1}. [c]273 K, 1 bar; unit of Q_{st}: kJ mol^{-1}

References

S1. R. Kagit, M. Yildirim, O. Ozay, S. Yesilot and H. Ozay, *Inorg. Chem.,* 2014, **53,** 2144-2151.
S2. M. G. Schwab, B. Fassbender, H. W. Spiess, A. Thomas, X. Feng and K. Mullen, *J. Am. Chem. Soc.,* 2009, **131,** 7216-7217.
S3. G. Li, B. Zhang, J. Yan and Z. Wang, *Macromolecules,* 2014, **47,** 6664-6670.
S4. A. K. Sekizkardes, S. Altarawneh, Z. Kahveci, T. İslamoğlu and H. M. El-Kaderi, *Macromolecules,* 2014, **47,** 8328-8334.
S5. W. C. Song, X. K. Xu, Q. Chen, Z. Z. Zhuang and X. H. Bu, *Polym. Chem.,* 2013, **4,** 4690-4696.
S6. P. Rekha, U. Sahoo and P. Mohanty, *RSC Adv.,* 2014, **4,** 34860-34863.
S7. T. Ben, C. Pei, D. Zhang, J. Xu, F. Deng, X. Jinga and S. Qiu, *Energy Environ. Sci.,* 2011, **4,** 3991-3999.
S8. K. T. Jackson, M. G. Rabbani, T. E. Reich and H. M. El-Kaderi, *Polym. Chem.,* 2011, **2,** 2775-2777.
S9. P. Mohanty and L. D. Kull, K. Landskron, *Nature Commun*., 2011, **2,** 401-406.
S10. Y. Zhu, H. Long and W. Zhang, *Chem. Mater.,* 2013, **25***,* 1630-1635.
S11. M. G. Rabbani and H. M. El-Kaderi, *Chem. Mater.,* 2012, **24***,* 1511-1517.
S12. S. Hug, M. B. Mesch, H. Oh, N. Popp, M. Hirscher, J. Senker and B. V. Lotsch, *J. Mater. Chem. A,* 2014, **2,** 5928-5936.
S13. M. Saleh and K. S. Kim, *RSC Adv.,* 2015, ***5***, 41745 - 41750.